JOURNAL OF AIRCRAFT
Vol. 42, No. 2, March–April 2005

Effect of Trailing-Edge Flap on a Tip Vortex

D. Birch* and T. Lee†
McGill University, Montreal, Quebec, H3A 2K6 Canada

The near-wake tip vortex flow structure behind a NACA 0015 airfoil with a trailing-edge flap was investigated. Lift-induced drag was computed based on vorticity and was compared with force-balance data. The vortex strength reached a maximum immediately behind the trailing edge and remained nearly constant up to two chord lengths downstream ($x/c = 3$). The displaced flap produced a more concentrated vortex of similar diameter and a higher induced drag compared to that of a baseline airfoil and had a larger radial gradient in circulation strength for flap angle $\delta \leq 15$ deg; the vortex radius increased significantly for $\delta = 20$ deg. For $\delta \leq 15$ deg, the axial flow velocity was jetlike with the peak values increased with the flap angle. The nearly symmetric vortex was observed at $x/c = 2.25$ for a displaced flap while at $x/c = 1.5$ for a baseline airfoil. The stength and interaction of the secondary and main vortices along the tip were also found to increase with the flap angle, and the vortex flow (immediately downstream of the deflected flap) was dominated by the presence of multiple vortices. The normalized circulation in the inner part of the symmetric vortex exhibited a self-similar structure, insensitive to the flap angle.

Nomenclature

b	=	wing span
C_{Di}	=	induced drag coefficient, $D_i/\frac{1}{2}\rho u_\infty^2 bc$
$C_{D,3\text{-d}}$	=	total drag coefficient of a three-dimensional wing configuration
$C_{L,2\text{-d}}$	=	lift coefficient of a two-dimensional wing configuration, lift/$\frac{1}{2}\rho u_\infty^2 bc$
$C_{L,3\text{-d}}$	=	lift coefficient of a three-dimensional wing configuration, lift/$\frac{1}{2}\rho u_\infty^2 bc$
c	=	airfoil chord
D_i	=	lift-induced drag
$D_{3\text{-d}}$	=	total drag of a three-dimensional wing configuration
Re	=	chord Reynolds number, $u_\infty c/\nu$
r	=	radial position
r_c	=	vortex core radius at which v_θ is equal to $v_{\theta\,\max}$
r_o	=	vortex outer radius
u_a	=	axial velocity
$u_{a,c}$	=	core axial velocity
u'_a	=	fluctuating axial velocity
u_∞	=	freestream velocity
v	=	spanwise mean velocity
v_θ	=	tangential or swirl velocity
w	=	transverse mean velocity
x	=	streamwise or axial direction
y	=	spanwise direction
z	=	transverse direction
α	=	angle of attack
Γ	=	vortex strength
Γ_c	=	core vortex strength
Γ_0	=	total circulation around vortex
δ	=	trailing-edge deflection angle
ζ	=	streamwise vorticity
ν	=	kinematic viscosity
ρ	=	density
σ	=	source term in Eq. (3)
ϕ	=	velocity potential
ψ	=	stream function

Received 27 November 2003; revision received 30 January 2004; accepted for publication 3 February 2004.

*Graduate Research Assistant, Department of Mechanical Engineering.
†Associate Professor, Department of Mechanical Engineering. Member AIAA.

I. Introduction

THE counter-rotating vortices generated by aircraft wing tips, because of their hazardous effects on flight safety and airport efficiency, continue to be of concern to aviation and aircraft manufacturers alike. Furthermore, a rotation of the freestream velocity vector gives rise to vortex drag. Moreover, tip vortices shed from helicopter rotor blades and propellers interact with following blades, causing rotor noise and vibration. Therefore, to minimize the separation time of aircraft during takeoff, as well as to reduce the tip vortex induced drag and noise, the tip-vortex wake characteristics must be measured and predicted accurately and reduced or eliminated, if possible.

Extensive investigations have been conducted to characterize the flow structure of the tip vortex and its dissipation or persistence, as well as its control in the mediate or far-field regions. Only limited experiments[1–8] had been conducted to investigate the dynamics of the initial rollup of a tip vortex around the wing tip and its subsequent development in the near field of a wing. The near-field behavior of a tip vortex is significant in both fixed- and rotary-wing aerodynamics, including the flow behind canard wings, helicopter blades (a major noise source), sails of submarines, and propeller blades. Devenport et al.[3] investigated the vortex structure in the range of 5–30 chord lengths downstream of a NACA 0012 airfoil with a blunt tip at $Re = 5.3 \times 10^5$ by using a miniature four-sensor hot-wire probe at $\alpha = 5$ deg and showed a deficit profile of approximately 0.84% of the freestream velocity u_∞. Chow et al.[4] investigated the tip-vortex flow (up to 0.678 chord lengths downstream of the wing) of a NACA 0012 airfoil model with a rounded tip at $\alpha = 10$ deg for $Re = 4.6 \times 10^6$ by using a seven-hole pressure probe and a triple hot-wire probe and indicated a peak axial velocity excess of approximately $1.7u_\infty$ at all measurement locations. Ramaprian and Zheng[5] observed no axial velocity excess or deficit for a tip vortex generated by a rectangular and square-tipped NACA 0015 wing at $\alpha = 10$ deg and $Re = 1.8 \times 10^5$ up to 3.3 chord lengths downstream. Despite much work, there is obviously still a need to improve our understanding of the behavior of the tip vortices in the near wake and their control. Moreover, the three-dimensional flow structure of a tip vortex is further complicated under the influence of a trailing-edge flap. An airfoil having its trailing-edge flap displaced becomes, in effect, a new airfoil having a different camber, and the downward deflected trailing-edge flap shifts the zero-lift angle α_0 negatively and increases the values of the lift and maximum lift coefficient.

The objective of this study was to characterize the effects of a trailing-edge flap on the near-field behavior a tip vortex (up to two chord lengths downstream of the trailing edge) of a square-tipped, rectangular NACA 0015 airfoil by using a miniature seven-hole

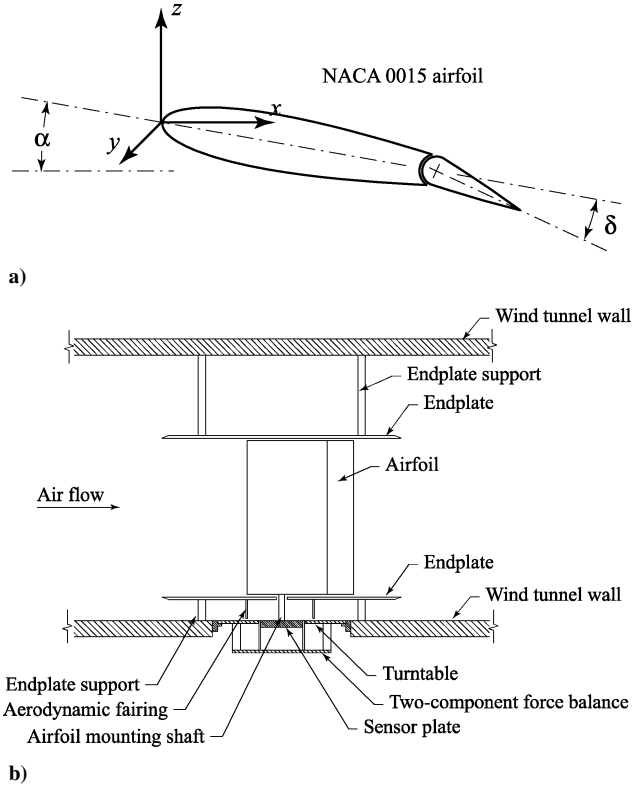

Fig. 1 Schematic of a) airfoil model and b) force-balance measurement system.

pressure probe and a cross-hot-wire probe. Special attention was given to the variation of the strength and size and the flow quantities of the tip vortex with the flap angle. Lift-induced drag was also computed and compared to the wind-tunnel force-balance data.

II. Experimental Apparatus and Methods

The experiments were carried out in the $0.9 \times 1.2 \times 2.7$ m suction-type subsonic wind tunnel with a freestream turbulence intensity of 0.08% at 35 m/s. A square-tipped, rectangular NACA 0015 airfoil, equipped with a full-span plain trailing-edge flap of a length of $25\%c$, with a chord $c = 25.4$ cm and a span $b = 37.9$ cm was used to generate the tip vortex (Fig. 1a). The trailing-edge flap angle was deflected downward and was set at $\delta = 0$–20 deg. The angle of attack α was the angle of attack of the forward part of the airfoil. The case of $\delta = 0$ deg is referred to as the baseline airfoil. The freestream velocity u_∞ was fixed at 12.3 m/s, which rendered a chord Reynolds number $Re = 2.01 \times 10^5$. The airfoil model was mounted vertically at the center of the bottom wall of the wind-tunnel test section. A miniature seven-hole pressure probe (with an outside diameter of 2.7 mm) and a cross-hot-wire probe were used to measure the mean and fluctuating velocity components. The pressure probe was calibrated in situ, following the calibration procedures described by Wenger and Devenport,[9] before the installation of the model. The pressure and hot-wire signals were sampled at 500 Hz, with a sampling time of 10 s, and were recorded on a Pentium II personal computer through a 16-bit A/D converter board. Probe traversing was achieved through a custom-built computer-controlled traversing system. Tip-vortex flowfield measurements were made at crossflow planes located between $x/c = 0.5$, 0.78, 0.9, 1.01, 1.03, 1.05, 1.07, 1.09, 1.15, 1.23, 1.3, 1.5, 1.75, 2.0, 2.25, and 3 for $\alpha = 10$ deg with

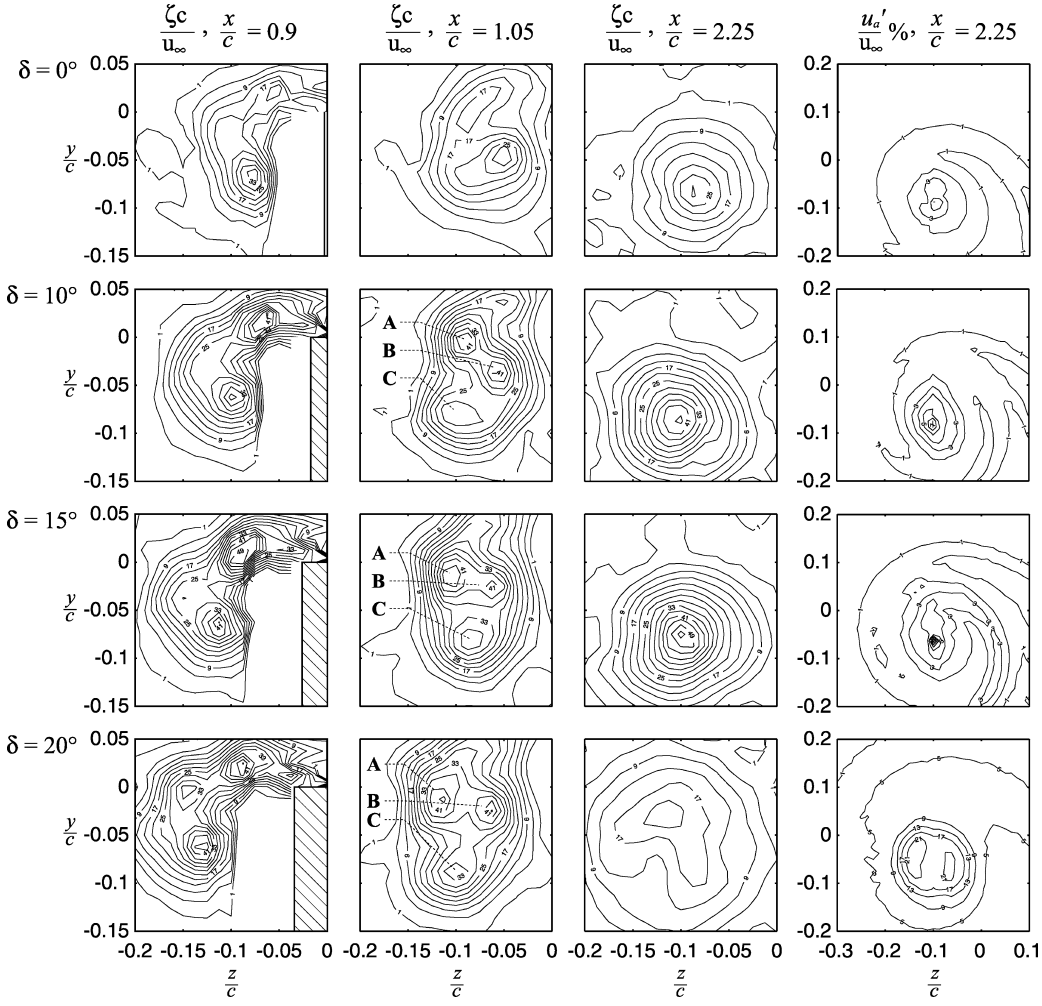

Fig. 2 Contours of streamwise vorticity and fluctuating axial velocity for α = 10 deg; numerical values denote $\zeta c/u_\infty$ or u_a'/u_∞ levels.

$\delta = 0$–20 deg. Data planes taken along the tip and in the near field of the wing model had 49×49 measuring grid points with an increment of $\Delta y = \Delta z = 3.2$ mm. Finer grid increments of $\Delta y = \Delta z = 1.6$ mm were also used in the determination of the vortex-core characteristics.

For lift and drag force measurements, the model was mounted vertically between two $0.45 \times 60 \times 60$ cm aluminum endplates with sharp leading edges and on an external two-component force balance located below the wind tunnel (Fig. 1b). The bottom plate was fixed to the bottom wall of the test section, and an aerodynamic fairing was placed around the shaft to isolate it from the tunnel flow. The top endplate was mounted on the top wall of the test section. The gaps between the airfoil and the endplates were kept at less than 1 mm to minimize leakage of flow through the gaps. This two-dimensional configuration approximated an airfoil with an effective aspect ratio of infinity. The two-dimensional wing configuration has total lift and drag coefficients $C_{L,2\text{-d}}$ and $C_{D,2\text{-d}}$, respectively. Furthermore, by removing the top endplate, the total lift coefficient $C_{L,3\text{-d}}$ and drag coefficient $C_{D,3\text{-d}}$ ($= C_{Dp} + C_{Di}$, where C_{Dp} is the profile drag coefficient and C_{Di} is the lift-induced drag coefficient) of a three-dimensional wing configuration were also obtained. The maximum experimental uncertainties in the results reported have been estimated as follows[8]: mean and fluctuating velocities 3.5%, vorticity component 8%, and vortex radius 4%. No wind-tunnel wall corrections were made to the present measurements.

III. Results and Discussion

A. Effect of Trailing-Edge Flap on Vortex Growth and Strength

Figure 2 shows the effect of a displaced flap on the streamwise mean vorticity $\zeta c/u_\infty$ and fluctuating axial velocity, u'_a/u_∞ contours at selected x/c for $\alpha = 10$ deg. Similar to the case of a baseline airfoil, the presence and rollup of the swirling secondary flows or vortices over onto the upper surface along the tip of the wing was also apparent for a flapped airfoil but with the strength increased with the flap angle. At $x/c = 0.9$, the structure reached the vicinity of the trailing edge and was positioned almost entirely above the upper surface. A well-organized and near-symmetric vortex flow with uniform spacing of the vorticity contours, except for the outermost part of the spiral, was observed at $x/c = 1.5$ (0.5 chords downstream of the trailing edge of the wing) for the baseline airfoil compared to $x/c = 2.25$ for $\delta \leq 20$ deg. Outside the core, the flow structure was dominated by the remainder of the wing wake, as can be seen clearly from the u'_a distributions. The near-symmetric tip vortex was, however, found to be more tightly wound, that is, with less diffusion, and with much higher vorticity levels, due to the flap-induced camber and increased lift, compared to that of a baseline airfoil. Also note that for a displaced flap, there was a presence of multiple vortices immediately downstream of the trailing edge (Fig. 3a), consisting of a main vortex (generated by the main body of the airfoil, vortex A) and a shear layer vortex (as a result of the rollup of the shear layers separated from the forward part of the airfoil, vortex B) of same rotation and approximately same strength and diameter, and a flap vortex (originated from the rollup of the shear layers separating from the displaced flap and with a higher core vorticity as a result of high concentration of circulation at the flap, vortex C). Figure 3a shows that, for $\delta = 15$ deg, vortex B merged into vortex C at $x/c = 1.15$ and lay on top of vortex A. At $x/c = 1.3$, vortex C merged into vortex A. The mutual induction and merging of the multiple vortices as they developed downstream for $\delta = 5$ and 15 deg are shown in Fig. 3b. As flap angle was increased, the convection rate of these vortices was found to increase with the increasing overall circulation, whereas the distance at which the vortices became completely merged remained relatively constant at $x/c \geq 1.3$.

The variation of the total vortex strength or circulation, $\Gamma_0/u_\infty c$, with x/c at $\alpha = 10$ deg and $\delta = 0$–20 deg, is summarized in Fig. 4a. The vortex strength was determined by employing the Stokes's theorem. Similar to the case of a baseline airfoil, Γ_0 increased rapidly along the tip and reached a peak value at $x/c = 1.05$ then remained basically constant ($\approx$95% of $\Gamma_{0,\text{peak}}$) for $1.3 < x/c < 3$, indicating that the integration path contained nearly all of the shed vorticity.

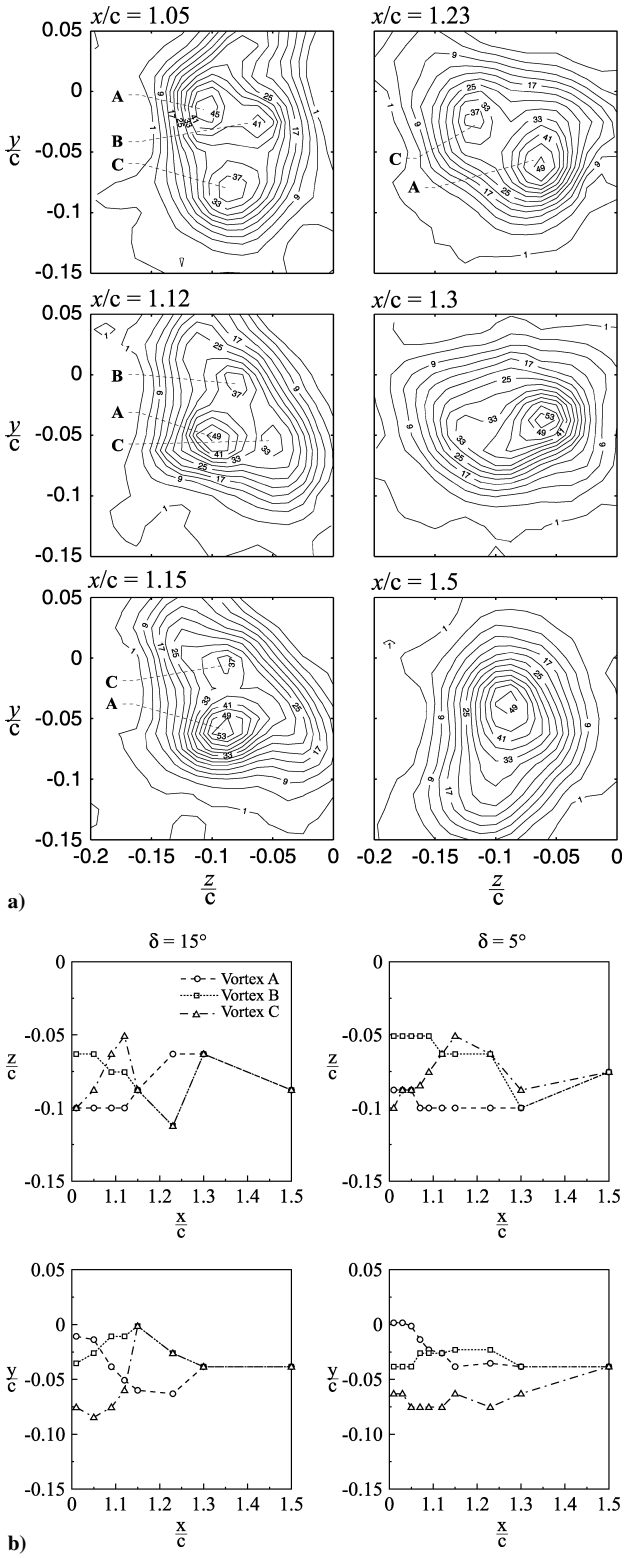

Fig. 3 Evolution of multiple vortices for α = 10 deg: a) vorticity contours for δ = 15 deg and b) vortex trajectory.

A peak value of $\Gamma_0/u_\infty c = 0.325$, 0.375, 0.46, and 0.52 [or about 90% of the bound vorticity Γ_b ($= 1/2 C_{L,2\text{-d}} c$) rolled up into the tip vortex] was found at $\delta = 5$, 10, 15, and 20 deg, respectively, compared to 0.25 (or less than 83% Γ_b) of the baseline airfoil. For $\delta = 20$ deg, however, the vortex strength was found to decay rather rapidly in the near wake due to massive separation at around the hinge line of the trailing-edge flap; a 15% reduction in the peak circulation strength was observed at $x/c = 2.25$. Figure 4a also shows that for

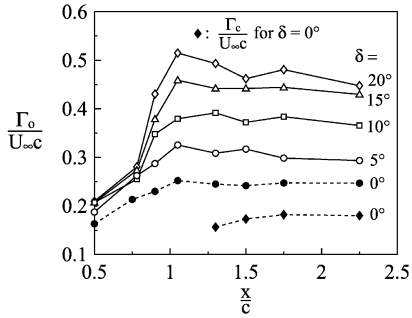

Fig. 4a Vortex strength with *x/c*.

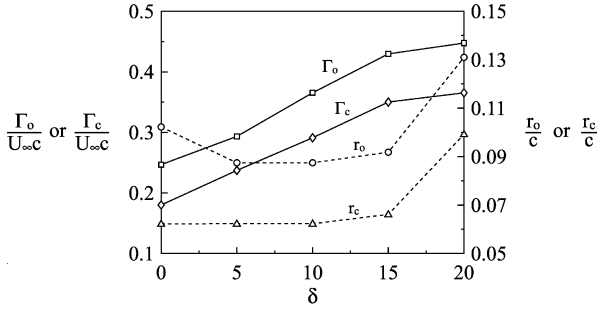

Fig. 4b Values of Γ_0, Γ_c, r_o, and r_c.

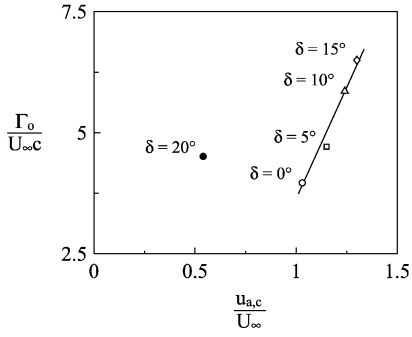

Fig. 4c Variation of Γ_0 with $u_{a,c}$ at *x/c* = 2.25 for α = 10 deg.

the baseline airfoil, the circulation at the core radius, Γ_c, remained essentially constant (≈74% of Γ_0) with the downstream distance, which is consistent with the theoretical value of $\Gamma_c/\Gamma_0 = 0.715$ of Lamb's solution,[10] whereas for a flapped airfoil, a ratio of Γ_c/Γ_0 of 82% was observed (Fig. 4b), that is, when a decaying vortex maintained geometric similarity, Γ_c/Γ_0 was constant. Figure 4a also shows that the growth and development of the main vortex was more significant along the tip with increasing flap angle. The total circulation of the main vortex increased approximately linearly along the tip (for $\delta \leq 5$ deg), whereas it increased nonlinearly and rapidly for larger deflection angles ($\delta > 5$ deg).

B. Effect of Trailing-Edge Flap on Vortex Flow Quantities

The influence of the flap angle on the various normalized flow quantities across the symmetric vortex core at $x/c = 2.25$ is shown in Fig. 5. The axisymmetric behavior of the tangential velocity v_θ and ζ in the inner region of the vortex and their decay to nearly zero in the outer part of the vortex, a characteristic of a well organized and nearly symmetric vortex, is apparent (Figs. 5a and 5b). For $\delta \leq 15$ deg, however, the displaced flap rendered a remarkable increase in the peak values of $v_{\theta\,\max}$, $\zeta_{\max}$, and $u_{a,c}$ (the core axial velocity) but with the core radius r_c (estimated by determining the distance from the point of $v_{\theta\,\max}$ to the vortex center) and u'_a remaining basically the same compared to those of a baseline airfoil (also Fig. 4b). At $\delta = 20$ deg, a significant increase in r_c and r_o (outer vortex radius) accompanied by a decrease in $v_{\theta\,\max}$, $\zeta_{\max}$, and u_a (wakelike) was observed, which further suggests that the flow was largely separated from the upper airfoil surface and that the axial turbulence u'_a had been increased by a large amount in the core and its rate of decay was correspondingly greater (Fig. 5d). Figure 5c shows that, for $\delta \leq 15$ deg, the axial velocity within the viscous wake produced islands of axial velocity that both exceeded and fell behind the free-stream value. The displaced flap, which produced a more concentrated vortex but of similar diameter (compared to those of a baseline airfoil), had a larger radial gradient in circulation strength (Fig. 6b). Also, the swirling-induced pressure drop along the vortex axis immediately behind the wing was strong enough to accelerate fluid from the wing tip area in the downstream direction and, therefore, generated the larger axial velocity. Note that, according to Bachelor,[11] the magnitude of the axial velocity in a trailing vortex is determined by a balance between the energy loss due to dissipation in the wing boundary layer and the radial gradient

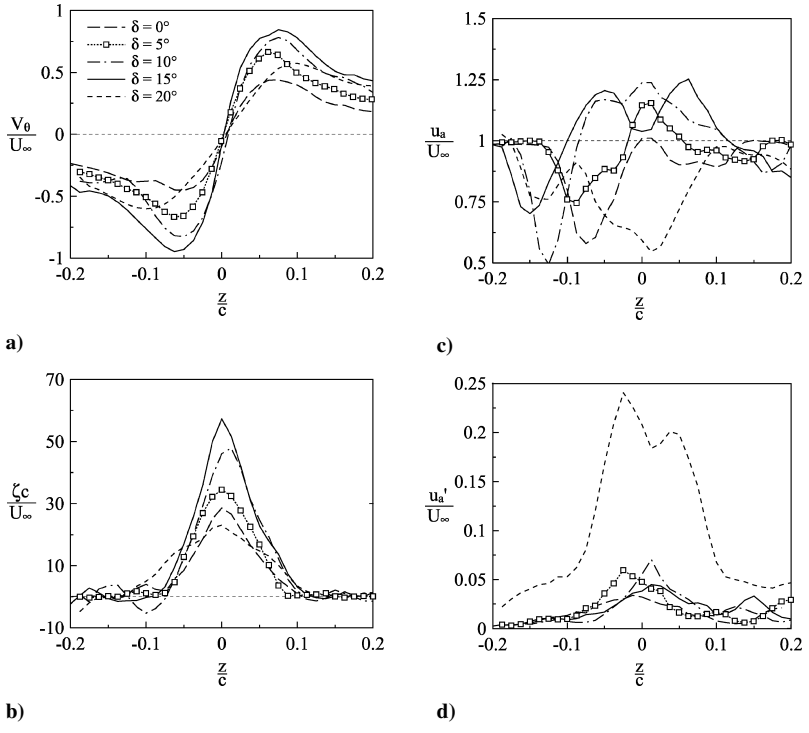

Fig. 5 Typical vortex flow structures across the vortex center at *x/c* = 2.25.

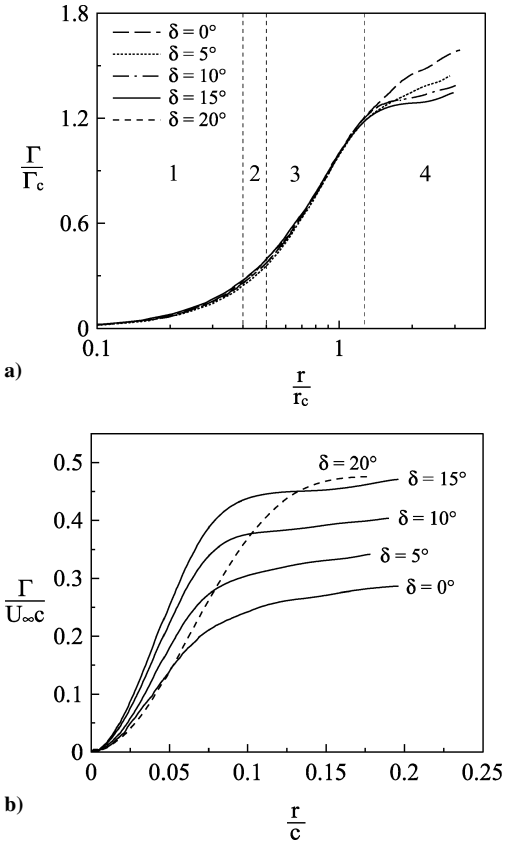

Fig. 6 Radial distribution of circulation at $x/c = 2.25$ for $\alpha = 10$ deg: 1, inner-core region; 2, buffer region; 3, logarithmic region; and 4, outer region.

in the circulation strength. The jetlike core axial velocity increased progressively with flap angle. An $u_{a,c}$ of $1.3u_\infty$ at $\delta = 15$ deg was found compared to a $u_{a,c} = 1.03u_\infty$ of a baseline airfoil (but with the majority of the axial velocity profile of wakelike). At $\delta = 20$ deg, the core axial flow became wakelike ($u_{a,c} = 0.54\%u_\infty$), a characteristic of an airfoil with a large separated wake. Furthermore, also note that scaling the circulation parameter by the vortex core radius collapsed the data from displaced flaps (except for $\delta \geq 20$ deg) to a single linear curve and a linear relationship between the core axial velocity and a nondimensional circulation parameter was indicated (Fig. 4c).

C. Self-Similarity of Inner Vortex Flow

It is known that in the near field the tip vortex soon after it is generated is highly three dimensional. However, the present measurements show that in the near wake a large inner region of the vortex rolled up quickly (Fig. 2) and that the layers of the spiral merged rigorously to result in a nearly axisymmetric structure of constant circulation (Fig. 4a) at 1.25 chord lengths downstream of the trailing edge for $\delta \leq 20$ deg. For $\delta = 0$ deg, however, the symmetric vortex structure was established earlier at 0.5 chords downstream. The radial distributions of vortex circulation, $\Gamma(r)/\Gamma_c$ vs $\log(r/r_c)$, at $x/c = 2.25$ for $\alpha = 10$ deg and $\delta = 0$–20 deg are presented in Fig. 6a. The distribution of circulation within the tip-vortex core followed a $\Gamma \propto r^2$ profile for $r/r_c < 0.4$ and varied logarithmically for $0.5 < r/r_c < 1.4$. For $r/r_c > 1.4$ (denoted region 4, Fig. 6a), the value of Γ continued to vary with r/c, which is attributed to that the rollup of the tip vortex was only nearly complete, and therefore, there was a slow addition of vorticity to the outer layers of the vortex from the shear layers arriving from the inboard regions (Fig. 6b). The observed self-similar or universal behavior of the inner region of a nearly axisymmetric tip vortex in the near-wake rejoin was found to be insensitive to the flap angle and is of particular interest because it generally takes a distance of several tens or even hundreds of wing chords downstream for the vortex to become fully developed and attain the characteristics of asymptotic turbulent trailing vortices. The empirical curve-fit relationships that describe the inner-core region and the logarithmic region for $0 \leq \delta \leq 20$ deg are[12,13] for $r/r_c < 0.4$

$$\Gamma(r)/\Gamma_c = 1.685(r/r_c)^2 \tag{1}$$

and for $0.5 < r/r_c < 1.4$,

$$\Gamma(r)/\Gamma_c = 2.092\log(r/r_c) + 0.980 \tag{2}$$

Moreover, all of the data within $0 < r/r_c < 1.2$ collapse onto a sixth-order polynomial (similar to that reported by Ramaprian and Zheng[5]): $\Gamma(r)/\Gamma_c = 1.733(r/r_c)^2 - 0.966(r/r_c)^4 + 0.225(r/r_c)^6$ with a correlation coefficient of 0.998.

D. Lift-Induced Drag

The lift-induced drag was computed[14] from the vorticity using the Maskell[15] induced-drag model. The vw crossflow velocity vectors within the measurement plane were decomposed into a stream function $\Psi(y, z)$ and a velocity potential $\phi(y, z)$ with the imposed boundary conditions requiring both Ψ and ϕ to be zero on the

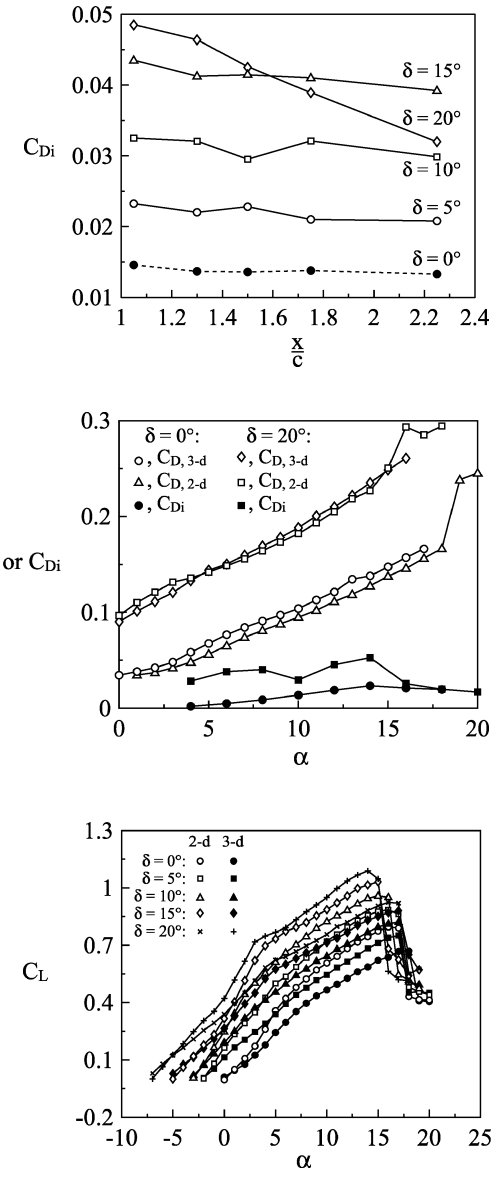

Fig. 7 Variation of induced drag with a) x/c at $\alpha = 10$ deg, b) α, and c) C_2.

edges of the measurement surface. The induced drag was then obtained by

$$D_i = \frac{1}{2}\rho_\infty \int\int_{S\zeta} \psi\zeta \, \mathrm{d}y \, \mathrm{d}z - \frac{1}{2}\rho_\infty \int\int_{S1} \phi\sigma \, \mathrm{d}y \, \mathrm{d}z \qquad (3)$$

where ζ is the vorticity, the surface S_ζ is the region within $S1$ (the surface at the measuring station) where the vorticity is nonzero, $\sigma (= \partial v/\partial y + \partial w/\partial z)$ is a source term, and the flow is incompressible. Figure 7a shows a summary of the values of the induced drag coefficient C_{Di} determined for a tip vortex in the near wake ($x/c = 1.05$–2.25). The values of C_{Di} increased with δ but varied slightly with x/c in the near-wake region (except for $\delta = 20$ deg). As expected, the airfoil with a displaced flap was found to generate much higher induced drag: Depending on the flap angle, a 160–320% increase in the induced drag was generated for $\delta \leq 15$ deg. For $\delta = 20$ deg, the induced drag was found to decrease considerably with the downstream distance in the near wake, a result consistent with the observed decrease in the vortex strength (Fig. 4a). Figure 7b indicates that, for $\delta = 20$ deg, the value of C_{Di} dropped drastically at $\alpha = 14$ deg and became comparable with the case of $\delta = 0$ deg. The induced drag was found to contribute to no more than 20% of the total drag of a three-dimensional configuration wing model, determined directly with a force balance at $Re = 2.01 \times 10^5$. The variation of C_L with α and δ is also presented in Fig. 7c.

IV. Conclusions

The effect of a trailing-edge flap on the vortex structure in the near wake behind a rectangular, squared-tipped NACA 0015 airfoil was investigated. In the near field, the details of the vortex structure were strongly influenced by the tailing-edge flap angle before attaining axisymmetry. The nearly symmetric vortex was observed for $x/c = 2.25$–3.0 with $\delta \leq 20$ deg compared to $x/c = 1.5$ for a baseline airfoil. When a decaying vortex maintained geometric similarity, Γ_c/Γ_0 was constant. The displaced flap produced a more concentrated vortex of similar diameter and had a larger radial gradient in circulation strength for $\delta \leq 15$ deg. The vortex radius increased significantly for $\delta = 20$ deg. Immediately downstream of the trailing edge, the tip vortex was dominated by the presence of multiple vortices. For $\delta \leq 15$ deg, the axial flow velocity was jetlike with the peak values increased with the flap angle. Scaling the circulation parameter by the vortex core radius had a linear relationship with the core axial velocity. The normalized circulation within the inner region of the nearly symmetric tip vortex exhibited a self-similar structure, insensitive to the flap angle. The induced drag increased with the flap angle. A maximum increase by as much as 320% was found at $\delta = 20$ deg due to the presence of massive flow separation induced by the deflected flap.

Acknowledgment

This work was supported by the Natural Sciences and Engineering Research Council of Canada.

References

[1]Francis, T. B., and Katz, J., "Observations on the Development of a Tip Vortex on a Rectangular Hydrofoil," *Journal of Fluids Engineering*, Vol. 110, 1988, pp. 208–215.

[2]Shekarriz, A., Fu, T. C., Katz, J., and Huang, T. T., "Near-Field Behavior of a Tip Vortex," *AIAA Journal*, Vol. 31, No. 1, 1993, pp. 112–118.

[3]Devenport, W. J., Rife, M. C., Liapis, S. I., and Follin, G. J., "The Structure and Development of a Wing-Tip Vortex," *Journal of Fluid Mechanics*, Vol. 312, 1996, pp. 67–106.

[4]Chow, J. S., Zilliac, G. G., and Bradshaw, P., "Mean and Turbulence Measurements in the Near Field of a Wingtip Vortex," *AIAA Journal*, Vol. 35, No. 10, 1997, pp. 1561–1567.

[5]Ramaprian, B. R., and Zheng, Y., "Measurements in Rollup Region of the Tip Vortex from a Rectangular Wing," *AIAA Journal*, Vol. 35, No. 12, 1997, pp. 1837–1843.

[6]McAlister, K. W., and Takahashi, R. K., "NACA 0015 Wing Pressure and Trailing Vortex Measurements," NASA TP-3151, 1991.

[7]Anderson, E. A., and Lawton, T. A., "Correlation Between Vortex Strength and Axial Velocity in a Trailing Vortex," *Journal of Aircraft*, Vol. 40, No. 4, 2003, pp. 699–704.

[8]Birch, D., and Lee, T., "Structure and Induced Drag of a Tip Vortex," *Journal of Aircraft*, Vol. 41, No. 5, 2004, pp. 1138–1145.

[9]Wenger, C. W., and Devenport, W. J., "Seven-Hole Pressure Probe Calibration Utilizing Look-Up Error Tables," *AIAA Journal*, Vol. 37, No. 6, 1999, pp. 675–679.

[10]Lamb, H., *Hydrodynamics*, 6th ed., Dover, New York, 1945, p. 592.

[11]Batchelor, G. K., "Axial Flow in Trailing Line Vortices," *Journal of Fluid Mechanics*, Vol. 20, 1964, pp. 645–658.

[12]Hoffmann, E. R., and Joubert, P. N., "Turbulent Line Vortices," *Journal of Fluid Mechanics*, Vol. 16, 1963, pp. 395–411.

[13]Phillips, W. R. C., "The Turbulent Trailing Vortex During Roll-Up," *Journal of Fluid Mechanics*, Vol. 105, 1981, pp. 451–467.

[14]Brune, G. W., "Quantitative Low-Speed Wake Surveys," *Journal of Aircraft*, Vol. 31, No. 2, 1994, pp. 249–255.

[15]Maskell, E., "Progress Towards a Method for the Measurement of the Components of the Drag of a Wing of Finite Span," Royal Aircraft Establishment, RAE Technical Rept. 72232, 1973.